UCLA
COMPUTATIONAL AND APPLIED MATHEMATICS

Vortex Ring Interaction by the Vortex Method

Christopher Anderson
Claude Greengard

March 1988

CAM Report 88-05

Department of Mathematics
University of California, Los Angeles
Los Angeles, CA. 90024-1555

VORTEX RING INTERACTION BY THE VORTEX METHOD

Christopher Anderson [1]
Department of Mathematics, University of California at Los Angeles
Los Angeles, CA 90024

Claude Greengard [2]
IBM Research Division, T. J. Watson Research Center
Yorktown Heights, NY 10598
and
Courant Institute of Mathematical Sciences, 251 Mercer St.
New York University, New York, NY 10012

1 Introduction

The vortex ring merger problem is a challenging one for numerical computation and is of considerable physical and mathematical interest. By the ring merger problem, we mean the flow which follows the simultaneous injection of two parallel vortex rings, identical in shape and in circulation, into an idle, incompressible fluid. We assume, for clarity of the discussion, that the vortex rings are generated in such a way that each by itself would move downward. At the edges which are closest together, the rings will tilt upward, and this causes them to move toward each other. After a short time, the rings appear to merge into one distorted vortex ring. Experiments have been carried out for a number of years. Photographic visualizations are reproduced in [17], for example. More recently, Schatzle and Coles have carried out further experiments, which have revealed considerably more detail, and in which they have measured a part of the vorticity field [19].

Of fundamental interest in this problem is the fact that the competition between the nonlinear vortex stretching process and the smoothing and damping by viscous stresses, which is thought to characterize turbulence, can be studied in reasonable isolation here. The problem is of further relevance due to the fact that concentrated tube-like structures appear in a variety of important flow situations (such as trailing vortices behind aircraft and hairpin vortices in three-dimensional boundary layers)

[1] Work partially supported by ONR Contract No. N00014-K-0727
[2] Supported at Courant by a NSF Mathematical Sciences Postdoctoral Fellowship.

where the topology of the structures can be seen to change in way similar to the ring merger process (filaments break and reconnect to filaments from other structures).

We shall discuss in this article applications of two different three-dimensional vortex methods to the problem. These methods are the vortex filament method, applied to inviscid (infinite Reynolds number) flow, and a random vortex method, applied to viscous (finite Reynolds number) flow. The vortex filament method we implement is similar to the one used by Chorin in [7]. The random vortex method we use was proposed in [2] as a slight improvement on Chorin's three-dimensional random vortex method [8]. The random vortex method seems to be a potentially useful candidate for the calculation of flows past solid boundaries in three dimensions (see [8] for a preliminary calculation by Chorin's algorithm).

Ring merger was first studied by use of a vortex method by Leonard in [16], where the rings were artificially broken and reconnected. Schwarz has used such an approach in his studies of superfluids [20], as has Buttke [6]. Recent numerical studies of reconnection in classical fluids can be found in the references [1,4,13,14,18,21]. The reader should be aware of the reference [15], which is a survey article on three-dimensional vortex methods.

For completeness, we recall that the governing equations (whose solutions we have sought to approximate) are the Navier-Stokes equations, which have the vorticity-velocity form

$$\frac{\partial \omega}{\partial t} + (\mathbf{u} \cdot \nabla)\omega - (\omega \cdot \nabla)\mathbf{u} = \nu \nabla^2 \omega$$

$$\mathbf{u}(\mathbf{x}) = -\frac{1}{4\pi} \int \frac{\mathbf{x} - \mathbf{y}}{|\mathbf{x} - \mathbf{y}|^3} \times \omega(\mathbf{y}) d\mathbf{y},$$

and the Euler equations, which correspond to the case $\nu = 0$ ($\mathbf{u}$ is the velocity field, ω is the vorticity field, and ν is the viscosity).

2 The Algorithms

2.1 The Vortex Filament Method

The vortex filament method we have implemented in our calculations is essentially the one used by Chorin [7]. It is a low-order version of an algorithm whose convergence has been proved [11]. The algorithm involves the approximation of the vortex rings at the initialization of the calculation by a family of filaments, each discretized by a finite number of particles. The set of particle positions at time t we denote by $\{\mathbf{x}_i(t); i =$

$1,\ldots,n\}$. The particles are initially chosen as follows. We lay down a rectangular grid on a vortex ring cross-section. We then rotate these grid points around the ring, in this way obtaining discrete filaments, which themselves discretize the vortex rings. Below, we designate by $\mathbf{x}_{j+1}(t)$ the position of the vortex element adjacent (oriented properly) to $\mathbf{x}_j(t)$. The vortex filament method involves the discretization in time of the family of ordinary differential equations

$$\frac{d\mathbf{x}_i}{dt}(t) = -\frac{1}{4\pi}\sum_{j=1}^{n}\left(\frac{\mathbf{x}_i(t)-\mathbf{X}_j(t)}{|\,\mathbf{x}_i(t)-\mathbf{X}_j(t)\,|^3}\right)_\varepsilon \times \boldsymbol{\Gamma}_j(t), \tag{1}$$

where

$$\mathbf{X}_j(t) = \frac{\mathbf{x}_{j+1}(t)+\mathbf{x}_j(t)}{2}, \tag{2}$$

$$\boldsymbol{\Gamma}_j(t) = \tilde{\Gamma}_j\frac{\mathbf{x}_{j+1}(t)-\mathbf{x}_j(t)}{|\,\mathbf{x}_{j+1}(0)-\mathbf{x}_j(0)\,|}, \tag{3}$$

and $\tilde{\Gamma}_j$ is the initial circulation of the vortex filament to which $\mathbf{x}_j, \mathbf{x}_{j+1}$ belong. The subscript ε appended to the Biot-Savart kernel means that this kernel is modified in a neighborhood of radius ε of the origin, in order that the singularity be removed:

$$\left(\frac{\mathbf{x}}{|\,\mathbf{x}\,|^3}\right)_\varepsilon = \begin{cases} \frac{\mathbf{x}}{\varepsilon^3|\mathbf{x}|} & \text{if } |\,\mathbf{x}\,| \le \varepsilon \\ \frac{\mathbf{x}}{|\mathbf{x}|^3} & \text{if } |\,\mathbf{x}\,| \ge \varepsilon \end{cases}$$

When computational elements become too widely separated, we interpolate new elements between such pairs; the formulas (1)–(3) for the velocity and vorticity remain unchanged (this is one particular convenience of the choice of approximations (1)–(3)).

2.2 The 3-D Random Vortex Method

For the simulation of viscous flows by vortex methods, diffusion operators are typically incorporated into the inviscid schemes, and the fluid evolution is approximated by a method of fractional steps: the inviscid equations are advanced over one time step, and this evolution is followed by an approximation of diffusion over the same time step; these steps are then repeated. Three different kinds of diffusion approximation have been proposed. These are: (*i*) the expansion of vortex cores; (*ii*) the solution of the heat equation at each step applied to the computational elements; and (*iii*) random walks of the vortex elements. The technique of core spreading is inconsistent with the Navier-Stokes equations. It was shown in [12] for two-dimensional flows that diffused vorticity is not correctly convected in the expanding core vortex

method. The errors are even worse in three dimensions, because such a scheme cannot properly take into account the history of the stretching. The idea (*ii*) is discussed in [10], to which the reader is referred for further discussion.

Random walks cannot be combined with the method described in Section 2.1 for the simulation of Navier-Stokes flow, because the evaluation of the vorticity depends on the relative positions of neighboring computational elements. If these positions were allowed to jump independently, the result would be an algorithm inconsistent with the Navier-Stokes equations. Consequently, Chorin [8] proposed a three-dimensional random vortex method in which segments of vorticity jump independently of each other. The vorticity of each segment is determined by the relative positions of the ends of the segments, just as in the vortex filament method.

An alternative approach was described in [2], in which the segments are replaced by individual particles. In order to describe this random vortex method, it is helpful first to define the computational velocity field $U[\mathbf{x}, \Gamma]$ associated to the set of vortex elements at positions $\mathbf{x}(t) = (\mathbf{x}_1(t), \ldots, \mathbf{x}_n(t))$ and with strengths $\Gamma(t) = (\Gamma_1(t), \ldots, \Gamma_n(t))$. We set, for $\mathbf{y} \epsilon \Re^3$,

$$U[\mathbf{x}(t), \Gamma(t)](\mathbf{y}) = -\frac{1}{4\pi} \sum_{j=1}^{n} \left(\frac{\mathbf{y} - \mathbf{x}_j(t)}{| \mathbf{y} - \mathbf{x}_j(t) |^3} \right)_\varepsilon \times \Gamma_j(t),$$

where now the Biot-Savart kernel is modified in a neighborhood of radius ε smoothly. Consider the family of ordinary differential equations

$$\frac{d\mathbf{x}_i}{dt}(t) = U[\mathbf{x}(t), \Gamma(t)](\mathbf{x}_i(t)) \tag{4}$$

$$\frac{d\Gamma_i}{dt}(t) = (\Gamma_i(t) \cdot \nabla) U[\mathbf{x}(t), \Gamma(t)](\mathbf{x}_i(t)). \tag{5}$$

In (5), the gradient is applied to U exactly. Given the configurations $\{\mathbf{x}_i(t), \Gamma_i(t)\}$, denote by $\tilde{\mathbf{x}}_i(t + \delta t), \tilde{\Gamma}_i(t + \delta t)$ the configuration obtained after one time step of a numerical approximation to equations (4), (5). Then we set

$$\mathbf{x}_i(t + \delta t) = \tilde{\mathbf{x}}_i(t + \delta t) + \eta_i$$

$$\Gamma_i(t + \delta t) = \tilde{\Gamma}_i(t + \delta t),$$

where the η_i are independent Gaussian random variables of mean zero and variance $2\nu\Delta t$. When the viscosity is set equal to zero, convergence to Euler's equations has been proved [5,9] for a higher order version of this algorithm.

As is the case for the vortex filament method, we need to improve the resolution by adding new elements when vortex stretching is present. Unlike the vortex filament

method, we do not have sequences of positions which represent filaments and which make interpolation natural. Rather, the random elements are all mutually independent. Thus, when an element stretches too much, we split it into two new elements, each with half the vortex strength, and which are separated in the direction of the vorticity. This splitting corresponds to the fact that the vorticity represented by the split elements has stretched in the vortex direction.

2.3 Comparison

To compare the two algorithms, let us consider the random vortex method for the case of zero viscosity (so that there are no random jumps). Given sets of positions and of vortex strengths at these positions, the convective velocities are calculated in similar ways in the two methods. Since the evaluation of the vorticity in the random method requires the differentiation of a computed velocity field, however, it might appear that the result should be much less accurate than vorticity evaluation in the filament method. However, the vorticity in the filament algorithm can be seen to be a finite difference approximation to the Lagrangian formula which expresses the evolution of vorticity in the random algorithm. Further discussion can be found in [2].

3 Computational Results

In the computations reported here, the cross-sectional radius of the rings was 0.02 while the ring radius was 0.1. The rings were initially tilted upward from the horizontal by 10 degrees. This tilting has the effect of inducing the collision between the two rings at an earlier time than if the rings were not tilted. The distribution of vorticity inside the rings was taken to be of uniform magnitude over the cross-section; smoother choices of the initial vorticity distribution led to similar results.

In figure 1, three perspective views of the results of an inviscid calculation at times $t = 0$, 8×10^{-4}, 16×10^{-4}, and 24×10^{-4} are plotted. The times steps used here were of size 2.5×10^{-5}. The rings were resolved with 49 filaments each, and each filament was initially resolved by 44 computational points. The value of ϵ was .014. For clarity, only nine of the filaments which form each ring are plotted. (If all were presented, the rings would look solid black.) The filament locations indicate the vorticity distribution. In the third column, only one of the vortex rings has been

plotted.

It is apparent from the plots that a great deal of core distortion develops in the rings. As the rings collide, those portions which are nearest to each other get pressed strongly together and flatten. From the perspective of the third column of figure 1, one sees that these portions have been greatly expanded in the vertical direction. Since these portions of the vortex tubes stretch greatly in the vorticity direction as well, it is clear from the incompressibility of the flow that they should flatten (as can be seen in the first column of figure 1). Discussion of the flattening and detailed views of the distorted vortex cores can be found in [1].

In figure 2, the results of a viscous calculation are presented. The initial configuration of the rings was the same as in the inviscid calculation. The coefficient of viscosity used here was $\nu = .005$, which corresponds to a Reynolds number, as it is usually defined in ring merger studies ($R = \Gamma/\nu$), of $R = 4000$. The vectors plotted in figure 2 are based at the locations of the computational elements, and their (scaled) magnitudes and directions are those of the vorticity vectors associated with those particles. For clarity, only a representative fraction of the total number of computational elements is shown.

Although the distribution of the vortex elements in figure 2 appears noisy, the corresponding velocity fields are surprisingly well behaved, and the flow field evolves in a laminar way. A helpful view of the computed flow can be obtained through the use of marker particles. These particles are initially distributed in the vortex rings. Their motion is calculated from the velocity field induced by the vortices (the markers are passive, however, and have no effect on the evolution of the flow). It is this type of visualization which is analogous to that seen in physical experiments when dye is used to indicate material parts of the fluid which initially lied within the vortex rings. In figure 3, the positions of the markers are shown at times corresponding to those in figure 2.

It is clear from figure 3 why the vortex rings are described as having merged. It is important to note, however, that the merger observed here is a merger only from the dye point of view. It is not clear from such a visualization how much vortex filament reconnection has taken place. Dye does not necessarily indicate the presence of substantial vorticity, and the lack of dye, especially, does not indicate an absence of vorticity. What is clear from from figure 3 (or from experimental dye visualizations) is only that enormous stretching is present in the central region as the rings are pulled apart. The action of viscosity does result in some cancellation of the vorticity, since the two adjacent edges of the vortex rings are of opposite circulation, but the relative

importance of the vortex stretching and diffusion, and the reconnection of vortex filaments, cannot be deduced from this visualization.

It is clear from the extreme pressing together of the cores (which occurs much faster than viscous time scales [4]) that many filaments must reconnect by the action of viscosity. Unfortunately, the large size of the smoothing parameter does not allow us to describe the vorticity field in sufficient, correct (from the point of view of numerical convergence) detail to permit a determination of the vortex strengths and the extent of viscous dissipation.

It is enlightening to compare figure 3 with figure 4, in which the configurations of marker particles at times corresponding to those in figure 3—but for the *inviscid* calculation—are plotted. Here, too, the marker particles have left the central region—but it is certainly not the case that the central vorticity has vanished and that reconnection has taken place. Indeed, since circulation must be preserved, the vorticity associated with the small amount of fluid in the central region is highly stretched and is greatly intensified in magnitude (although, of course, the circulation is preserved).

The results presented in this article were calculated with a fixed value of ϵ. They do not represent converged solutions of the equations of motion. Smaller values of the smoothing parameter require substantial increases in the number of computational elements, which exhaust computer resources. However, the features we have described are independent of ϵ. This question is discussed further in [3], where computational results are presented for a range of values of the smoothing parameter. We present, for comparison, one final plot in figure 5 of the calculated dye evolution for a random vortex method computation with the parameters as above, except for a larger value of the smoothing parameter, $\epsilon = .02$.

4 Discussion

The calculations reported here suggest certain implications for other work on ring merger and on related vortex tube interactions. One of these concerns the very small scales, which, as we have seen, arise in a very short time. Fluid mechanical calculations most typically involve grid-based schemes. The possible resolution which can be achieved with such schemes is clearly limited by the grid lengths. If the development of these small scales is a generic phenomenon, it will be very difficult to calculate accurately the details of the pressing together, and diffusion, of vortex

tubes with an Eulerian scheme, not only for inviscid, but for high Reynolds number flows as well.

Secondly, vortex ring merger has often been thought of, and sometimes modelled, as an interaction of vortex tubes of circular cross-section in which the vortex filaments of which these tubes are comprised break and reconnect when the approach is sufficiently close. However, we find that the vortex ring cores deviate very much from their initially circular shapes. Calculations discussed in [1] reveal that the cores do not become uniformly pressed against each other at infinite Reynolds number. The form of the core deformations suggests that the nature of the reconnection must depend on the Reynolds number, that some of the filaments—those which are pushed most closely together by the convection, and which then diffuse and cancel—reconnect much sooner than the others. Thus, perhaps the reconnection process is too subtle to admit representation by a universally valid model.

In the future, more detailed computations of the high Reynolds number flow will become available, we hope, which will allow a better understanding of the nature of the reconnection process.

References

[1] Christopher Anderson and Claude Greengard. Core flattening, reconnection, and the possibility of singularity in the ring merger problem. Preprint.

[2] Christopher Anderson and Claude Greengard. On vortex methods. *SIAM J. Numer. Anal.*, 22(3):413–440, 1985.

[3] Christopher Anderson and Claude Greengard. The vortex ring merger problem at infinite Reynolds number. Preprint.

[4] W. T. Ashurst and D. I. Meiron. Numerical study of vortex reconnection. *Phys. Rev. Lett.*, 58:1632, 1987.

[5] J. Thomas Beale. A convergent 3-d vortex method with grid-free stretching. *Math. Comp.*, 46:401–424, 1986.

[6] Thomas F. Buttke. *A numerical study of superfluid turbulence in the self-induction approximation.* PhD thesis, U. Calif. Berkeley, 1986.

[7] Alexandre Joel Chorin. The evolution of a turbulent vortex. *Comm. Math. Phys.*, 83:517–533, 1982.

[8] Alexandre Joel Chorin. Vortex models and boundary layer instability. *SIAM J. Sci. Stat. Comput.*, 1:1–21, 1980.

[9] G. H. Cottet. A new approach for the analysis of vortex methods in two and three dimensions. *Ann. Inst. H. Poincaré.* To appear.

[10] G. H. Cottet and S. Mas-Gallic. A particle method to solve transport-diffusion equations. Part II: the Navier-Stokes system. Preprint.

[11] Claude Greengard. Convergence of the vortex filament method. *Math. Comp.*, 47:387, 1986.

[12] Claude Greengard. The core spreading vortex method approximates the wrong equation. *J. Comput. Phys.*, 61(2):345–348, 1985.

[13] Claude Greengard. *Three-Dimensional Vortex Methods.* PhD thesis, U. Calif. Berkeley, 1984.

[14] S. Kida and M. Takaoka. Bridging in vortex reconnection. *Phys. Fluids*, 30:2911–2914, 1987.

[15] A. Leonard. Computing three-dimensional incompressible flows with vortex elements. *Annual Rev. Fluid Mech.*, 17:523–559, 1985.

[16] A. Leonard. Numerical simulation of interacting three dimensional vortex filaments. In R. D. Richtmeyer, editor, *Proc. 4th Int. Conf. on Num. Methods in Fluid Dynamics*, pages 245–250, Springer-Verlag, 1975.

[17] Y. Oshima and S. Asaka. Interaction of two vortex rings along parallel axes in air. *Jour. Phys. Soc. Japan*, 42:708–713, 1977.

[18] Alain Pumir and Robert M. Kerr. Numerical simulation of interacting vortex tubes. *Phys. Rev. Lett.*, 58(16):1636–1639, 1987.

[19] Paul Schatzle. *An Experimental Study of Fusion of Vortex Rings.* PhD thesis, California Institute of Technology, 1987.

[20] K. W. Schwarz. Three-dimensional vortex dynamics in superfluid ^{4}He: Line-line and line-boundary interactions. *Phys. Rev. B*, 31:5782, 1985.

[21] Karim Shariff. *Dynamics of a Class of Vortex Rings.* PhD thesis, Stanford Univ., 1988.

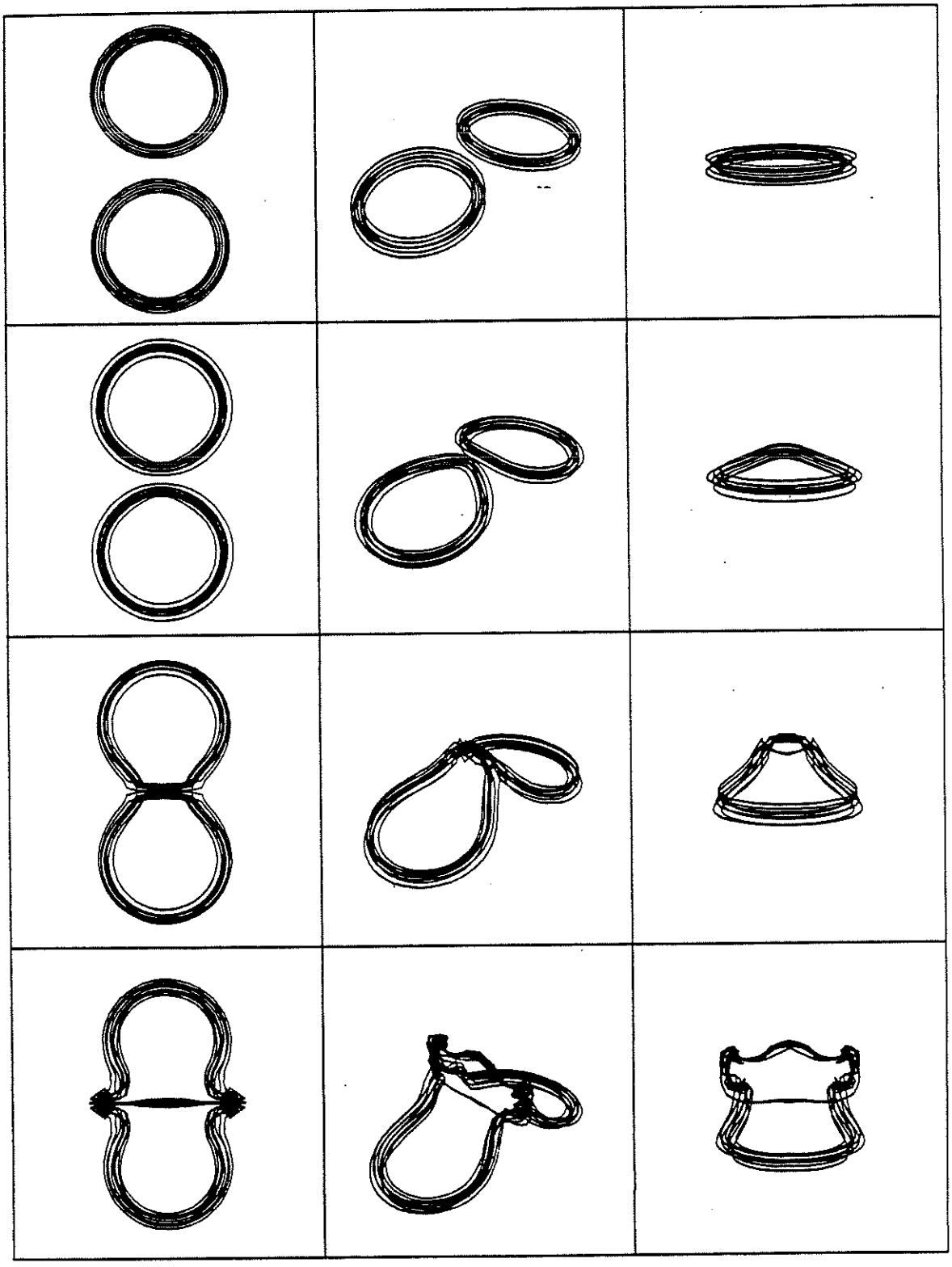

Figure 1: Inviscid evolution of vortex filaments.

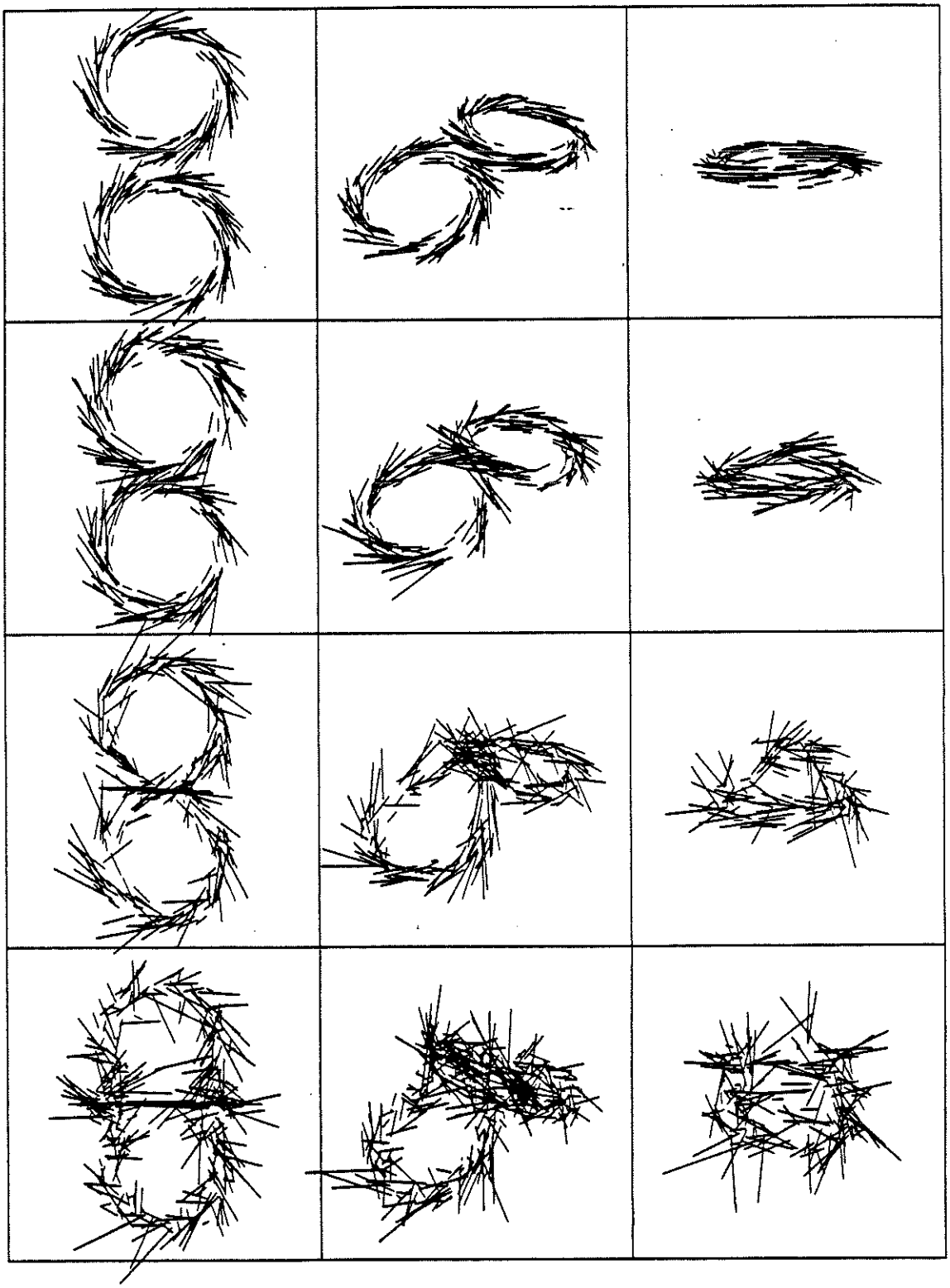

Figure 2: Evolution of computational vorticity vectors by the random vortex method.

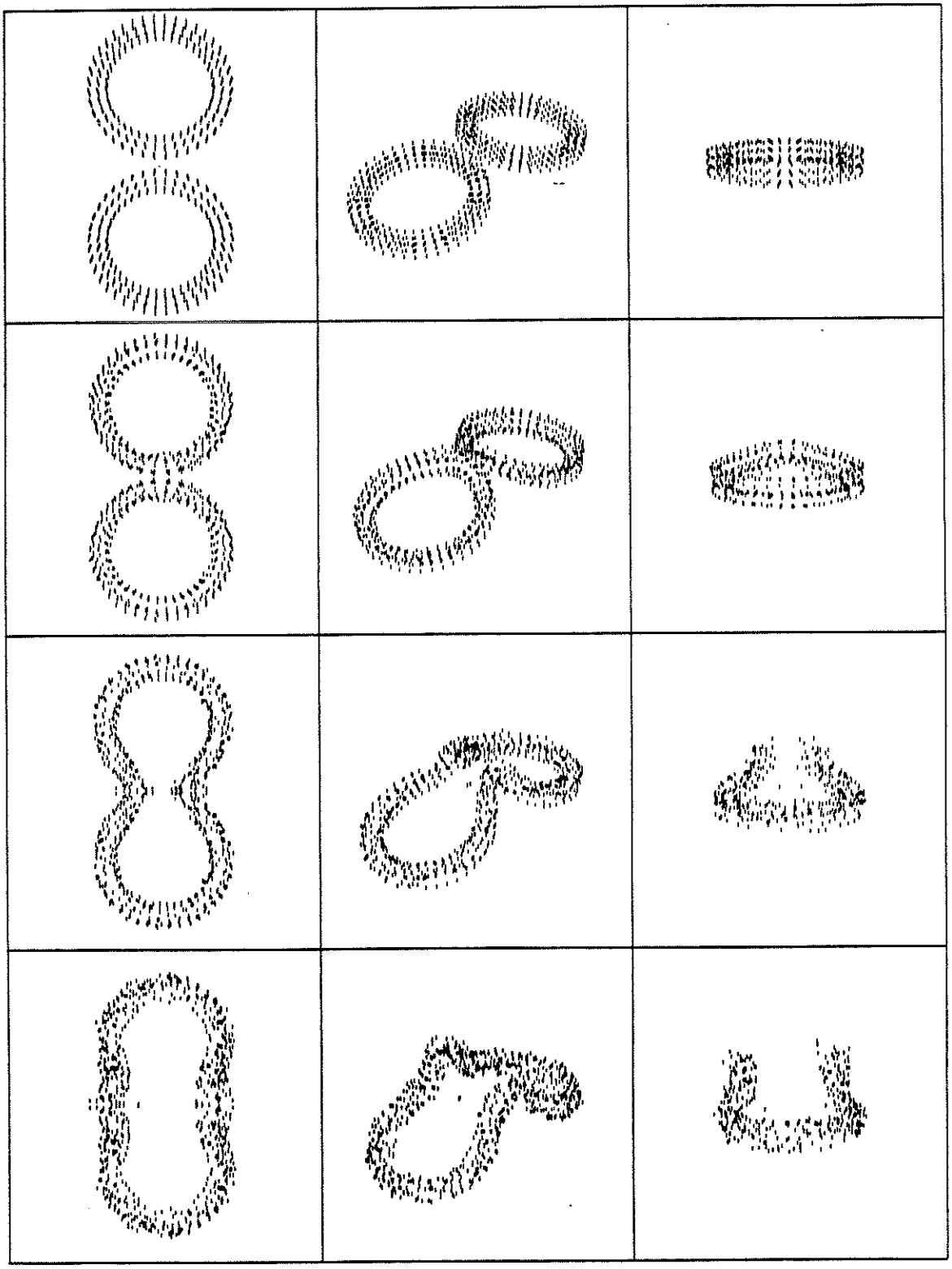

Figure 3: "Dye" visualization of the random vortex method calculation.

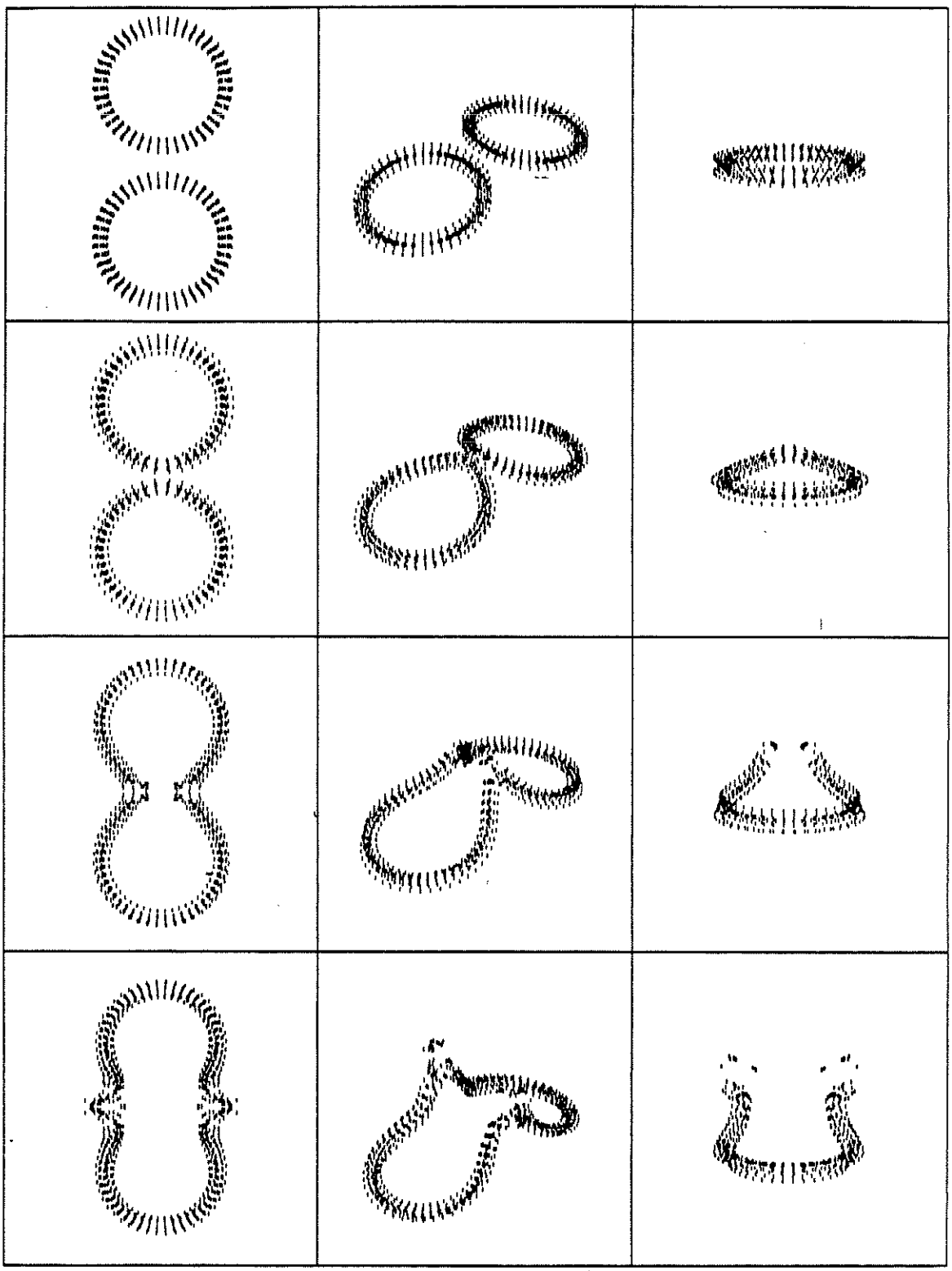

Figure 4: "Dye" visualization of the inviscid calculation.

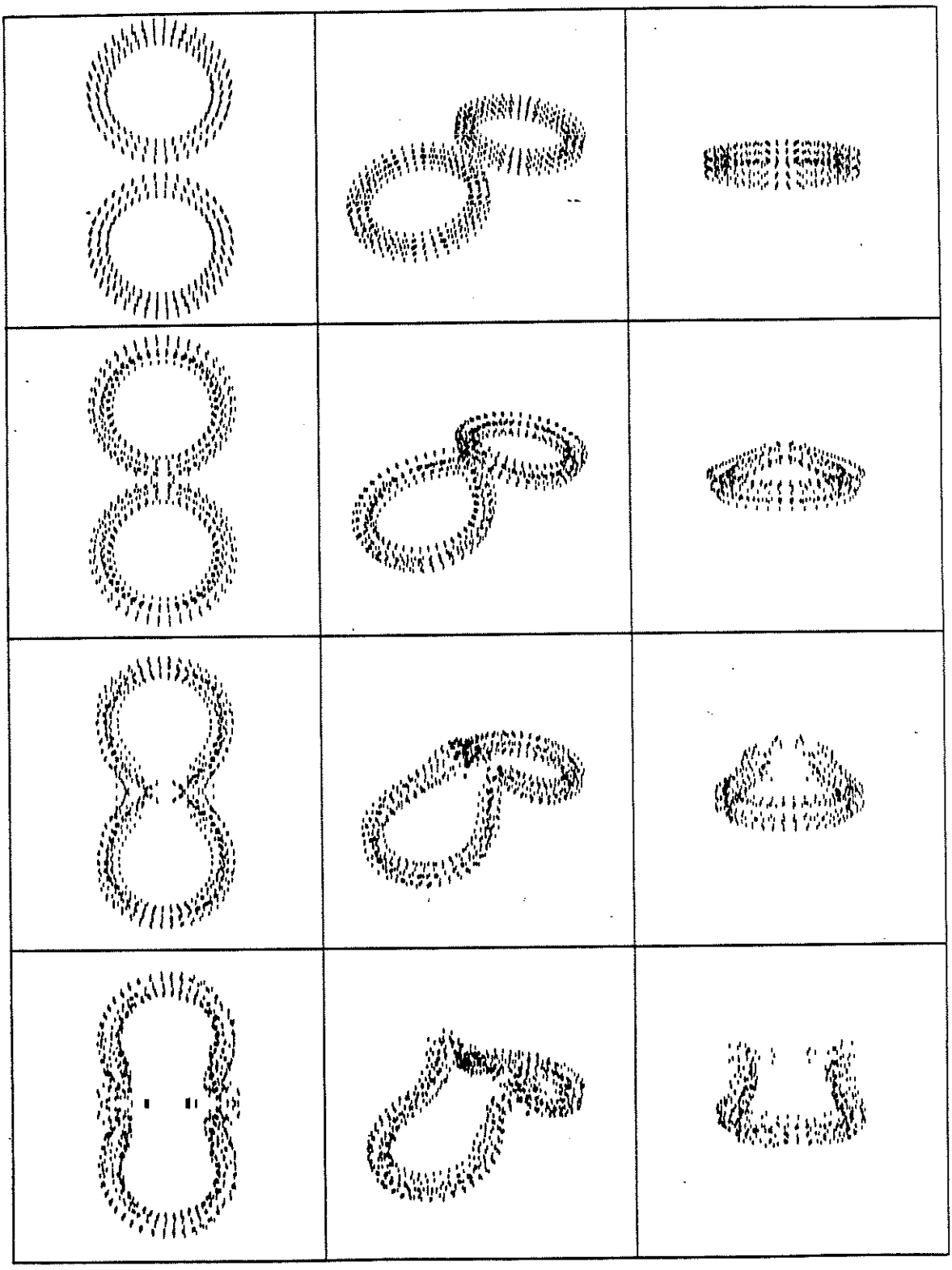

Figure 5: "Dye" visualization of the random vortex method calculation with $\epsilon = .02$.